Geoscience Frontiers 9 (2018) 471–483

Contents lists available at ScienceDirect

China University of Geosciences (Beijing)

Geoscience Frontiers

journal homepage: www.elsevier.com/locate/gsf

Research Paper

Early Holocene climate signals from stable isotope composition of ice wedges in the Chara Basin, northern Transbaikalia, Russia

Yurij K. Vasil'chuk [a,*], Alla C. Vasil'chuk [a], Julia V. Stanilovskaya [b]

[a] Geography and Geology Departments, Lomonosov Moscow State University, Moscow, Russia
[b] Sergeev Environmental Geoscience Institute of the Russian Academy of Sciences, Russia

A R T I C L E I N F O

Article history:
Received 3 October 2016
Received in revised form
4 April 2017
Accepted 28 April 2017
Available online 17 May 2017
Handling Editor: Wen-Jiao Xiao

Keywords:
Holocene
Ice wedge
Stable isotopes
Southern permafrost areas
Northern Transbaikalia

A B S T R A C T

Stable isotope composition of syngenetic and epigenetic ice wedges, radiocarbon age, and pollen spectra of the surrounding deposits were studied during long term investigations at the "Belyi Klyuch" site on the first (6–8 m height) terrace of the Chara River (720 m.a.s.l.) in northern Transbaikalia to assess climatic conditions during ice-wedge formation. It was revealed that Holocene ice wedges had been formed from 10 to 7.5 ka ^{14}C BP. The isotope composition (δ^{18}O, δ^{2}H) of relict ice wedges is the lightest and amounts −23‰ and −185‰, correspondingly. The isotopic compositions of ice lenses from sandy loam above ice wedges are −15.7‰ and −133‰; of small ice wedge in peat and sand are −15.3‰ and −117.9‰, accordingly.

Interpretation of the ice wedge isotope composition has yielded that mean winter temperatures during cold stages of Holocene optimum were lower than today, during warm stages they were close to modern ones. During the coldest stages of Holocene optimum the total annual freezing index varied from −5100 to −5700 °C degree days, i.e. 300–600 °C degree days colder than during extremely severe modern winters. The total annual thawing index varied from 1300 to 1800 °C degree days, which was slightly higher than modern ones.

1. Introduction

Ice wedges can be a valuable source of proxy information on past climates (Vasil'chuk, 1992, 2013). The stable-isotope signature (δ^{18}O and δ^{2}H) of syngenetic ice wedges is an important indicator in long-time-scale paleoclimatic reconstructions according to the empirical linear relationship between mean winter and mean January air temperature and the isotopic composition of wedge ice (Vasil'chuk, 1992) as the snow melt water is the main source for ice-wedge formation. The isotopic signature of winter precipitation is transferred to ice wedges. As the winter precipitation originates from the air mass, it provides a site-specific signature of the ambient air temperature, stored within ice wedges at the site. This means that a major shift in the isotopic composition of different elementally ice veins could reflect the paleotemperature fluctuation. The linear relationship between mean winter temperatures and the isotopic composition of ice wedges permits quantitative reconstruction of paleotemperature during the ice-wedge growth.

Patterned ground and ice wedges are widespread within the Chara Basin in northern Transbaikalia (57°N and 118°E) especially within sediments of the first terrace of the Chara River (Lopatin, 1967). Sediments of the first terrace are medium and coarse sands, often interbedded with gravel and pebbles. It is supposed that ice wedges in pebbles and gravels may form only in extremely severe winter conditions (Black, 1965). Ice wedges in the Chara River valley are valuable as analogues of ice wedges formed in severe conditions in gravel sediments.

Age of ice wedges assessed indirectly by their location in the first terrace sediments in river valley. This led to the erroneous opinion, that ice wedges are Late Pleistocene relict, as buried wedge ice in the northern part of the Udokan Range at the height of 900–1000 m was dated at least to the Late Pleistocene (Romanovsky et al., 1988), which is significantly more severe than Holocene. It was assumed that the conditions for the ice-wedge formation were significantly more severe than modern and Holocene ones based on their formation in gravel sediment. We obtained data that are redefining the age of ice wedges and clarifying the temperature conditions of their formation. The main objective of the study is to get Holocene paleotemperature signal from ice wedges in the first terrace of the Chara River.

* Corresponding author.
E-mail address: vasilch_geo@mail.ru (Y.K. Vasil'chuk).
Peer-review under responsibility of China University of Geosciences (Beijing).

http://dx.doi.org/10.1016/j.gsf.2017.04.008

Ice wedges can be a valuable source of proxy information on past climates (Vasil'chuk and Vasul'chuk, 1995; Vasil'chuk et al., 2000; Opel et al., 2011; Yang and Jin, 2011; Yang et al., 2013, 2016). The main objective of the study is to get Holocene paleotemperature signal from ice wedges in the first terrace of the Chara River.

2. Study area

The study area is located in the southern part of Siberian Platform within the Chara Basin (708–740 m.a.s.l., Fig. 1). The eastern part of the basin is limited by the Udokan Ridge (2515 m.a.s.l.), the west part by the Kodar Ridge (3073 m.a.s.l.). Chara Basin has a length of up to 125 km; maximum width in the middle part is 35 km. The slopes and bottom of the basin are occupied by numerous mountain ridges, alluvial fans, river terraces; some part of the territory is swamped. The main landscapes are marshy meadows, dwarf birch, pine forests and mountain taiga.

The climate is continental with a winter temperature inversion and the predominance of western (regional) atmospheric transport. Heterogeneous distribution of meteorological elements within the basin is caused by the imbricate location of the ridges.

The observations carried out for more than 70 years at the meteorological station of Old Chara village. Meteorological data allow allocating a period of relative cooling (1939–1960) and a period of relative warming (1960–2004) (Weather of Russia…, http://meteo.infospace.ru). The average air temperature for 1959–2015 in Chara Basin was −7.6 °C, minimum (−9.8 °C) was recorded in 1969, the maximum (−3.6 °C) in 2004 (Fig. 2). Average winter temperature for 1939–1960 was −21 °C and the average January temperature was −34 °C (Climate reference book…, 1966), the average January temperature for 1960–2004 was −33 °C. We emphasize that the annual freezing index for 1939–1960 was 4438 °C degree days. It is lower by 100–130 °C degree days than for 1960–2004. The annual thawing index is 1633 °C degree days (Weather of Russia…, http://meteo.infospace.ru).

Annual amplitude of the air temperature is 92 °C: absolute minimum is −57 °C; the absolute maximum is +35 °C. Period with negative mean monthly temperature lasts 7–8 months. Daily amplitude is 27–37 °C, which is associated with intense sun exposure during daytime and the intensive radiance of the surface at night. The absolute minimum recorded in July in the Chara village is −2 °C. Sharp daily fluctuations with significant temperature decreases at night lead to occasional freezing events in July (Plyukhin, 1990).

The precipitation increased from 220 mm (1973) to 450 mm (1989), and to 420 mm (1993) has been observed. Average precipitation during last 50 yr is 340 mm. The duration of snow cover in the basin averages 176 days, and average snow depth varies from 15 to 20 cm, its maximum height according to the Chara meteorological station is 30 cm, the minimum is 6 cm. Wind transport is negligible, which is favorable for the ubiquitous uniform cooling of different elements of the relief (Nekrasov and Zabolotnik, 1967). The warming effect of snow is very high, so cooling during dry winters and following cracking are very intensive. Temperature gradient in snow is 1.5°/cm or more (Kolomyts, 1966). Due to the friability and high heat insulating ability of the snow cover the active layer is completely frozen by February; by this time of winter, obviously, the most active frost cracking occurs.

Seasonal thawing on the terraces and flood plain begins in early May and ends in October. Active layer depth varies from 0.5 to 3.5 m (Zabolotnik and Klimovsky, 1966). The minimum depth of thawing (up to 1 m) has been recorded the treeless marshy areas or in areas with sparse larch forest, therefore, these sites are the most favorable for the development and preservation of ice wedges.

The mean annual soils temperature (as measured in 1964) was relatively high and ranging from −2 °C under a canopy of larch woodlands to positive values of 1–2 °C on dry sand and in the dry open field (Gavrilova, 1967). Similar range was determined by our measurements in 2007–2014. Contrast of permafrost conditions, even within a single element of the relief, is very noticeable; the average soil temperature can vary by 2 °C and more. This contrast is even more emphasized, for example, with Upper Chara thermal chloride-sulphate-sodium spring with a temperature of 41 °C in April to 50.5 °C in the northern part of the Chara Basin near Arbakalir Lake in May (Nekrasov and Golovanova, 1966).

The spatial distribution of permafrost in Chara region varies from sporadic to continuous. Taliks locate within the Chara Sandy Desert on the left bank of the Chara River and under the beds of large rivers (Chara, Nizhniy Ingamakit, Sredniy Sakukan and others). The Chara Basin is surrounded by mountains where the relief changes from smooth and rounded to typical alpine with present-day glaciation. Numerous permafrost features are present, including kurums,

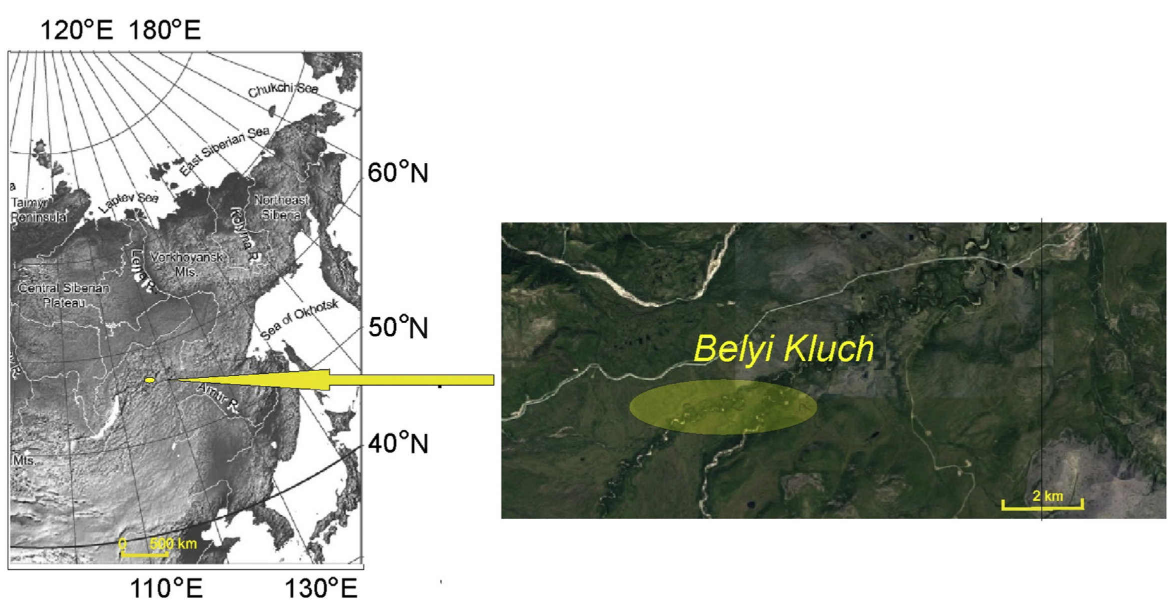

Figure 1. Location of the study site along the Transbaikalia.

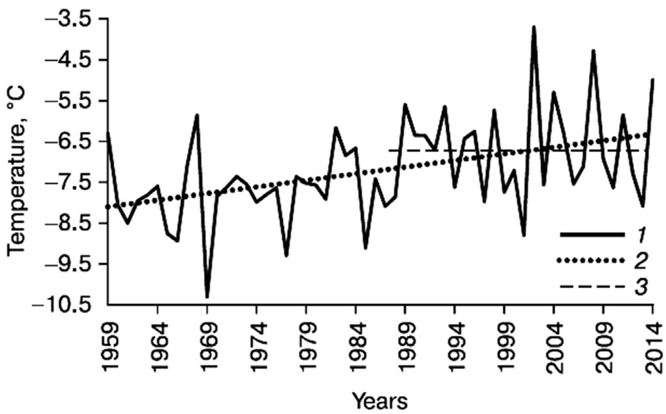

Figure 2. Mean annual air temperatures at the Chara meteorological station, averaging from September to August (from Sergeev et al., 2016). 1 – The temperature course; 2 – the linear trend for the period of 1959–2014; 3 – the linear trend for the period of 1988–2014.

thermokarst landforms, icings, patterned ground, frost mounds, and solifluction lobes (Romanovsky et al., 2010).

3. Methods

3.1. Study of deposits and ground ice

The "Belyi Klyuch" exposure (56.766°N, 118.103°E) with large ice wedges located within the first (8-m-high) terrace on the right bank of the Chara River, 5 km from Novaya Chara settlement was investigated in 1985, 1988, and 2006–2009 (Figs. 3 and 4 and Supplementary Fig. S1).

Structure of the first terrace deposits of the Chara River in different parts of the exposure varies distinctly. Coarse sand layer occurs near the surface but in some cases, peat or fine-grained sediment covers it. Lithological differences in structure of different parts of the terrace detect different facies conditions during the terrace formation. Lithological differences are largely responsible for variations in the structure of ice wedges in different sediments. However, the presence of ice wedges in fine-grained sediments interbedded with pebbles and gravel (Supplementary Fig. S2) is the most important though the ice-wedge polygons are not visible on the terrace surface.

3.2. Radiocarbon dating

Samples of organic material for radiocarbon age determination have been selected in several parts of 8-m terrace (Table 1). ^{14}C ages have been obtained in Radiocarbon Laboratory of GIN RAS (L.D.Sulerzhitsky) and in Radiocarbon Laboratory of the Institute of Geology of Estonia (R.A.Rayamyae). The obtained conventional ^{14}C ages were calibrated using the IntCal13 calibration curve (Reimer et al., 2013).

3.3. Palynological analysis

Pollen analysis of Holocene sediments in Chara Basin containing ice wedges was done by Vasilyeva (Klimovsky and Vasilyeva, 1967). Our interpretation of these data allowed estimating changes in summer temperatures (A.Vasil'chuk, 2007) during terrace deposits accumulation (Supplementary Table S1).

3.4. Isotopic analysis

Authors sampled ice wedges and lenses of segregated ice from the surrounding sediments in different years. Stable isotope concentration is usually expressed in ppm relative values (‰) and denoted by the Greek letter δ (δ^{18}O and δ^{2}H). As the zero reference for measuring ^{2}H and ^{18}O, Vienna Standard average ocean water

Figure 3. The 6- to 8-m-high Chara River terrace. 7, 8, 9 and 10 are locations and numbers of ice wedges within the bluff.

Figure 4. Ice wedges in sand and gravel deposits interbedded with pebbles in the bluff of the 6 to 8-m Chara River terrace: wedge 4 (a) – photo by V.N.Zaytsev, 1985; wedge 7 (b) – photo by D.O.Sergeev, 2006.

Table 1
Radiocarbon ages from the organic plant material from the ice wedge surrounding deposits in the 6–8 m Chara River terrace in 1985 and 1988 sampling years.

Sample No.	Depth (m)	Material	Lab ID	^{14}C age (yrs BP)	Calibrated age ranges [cal yrs BC] 1σ confidence interval
353-YuV/1	1.5	Wood	GIN-5706	7840 ± 60	7024–6508
353-YuV/2	1.5	Peat	GIN-5709	7570 ± 250	7072–5928
353-YuV/14	4.7	Peat	GIN-5707	9150 ± 80	8571–8242
353-YuV/15	4.7	Wood	GIN-5708	9740 ± 60	9313–8864
3-85-36	4.65–5.0	Plant fragments	Tln-1284	9450 ± 70	9127–8561
3-85-5	2.2	Plant fragments	Tln-1283	8875 ± 65	8242–7761
3-85-5	3.2	Plant fragments	Tln-1290	8980 ± 80	8317–7837
3-85-33	4.5	Wood	Tln-1295	9610 ± 80	9243–8776
3-85-32	1.2–1.3	Wood	Tln-1274	8350 ± 65	7545–7149
3-85-32	3.2	Wood	Tln-1273	9230 ± 40	8562–8312
3-85-32	3.4	Wood	Tln-1275	9180 ± 40	8537–8292
3-85-28-5	2.15	Wood	Tln-1294	8350 ± 60	7544–7191
3-85-28-5	2.15	Peat	Tln-1309	8035 ± 55	7137–6707
3-85-28-5	2.6	Wood	Tln-1291	8500 ± 80	7680–7355
3-85-28-5	3.5	Wood	Tln-1296	9260 ± 55	8625–8316
3-85-28-5	3.5	Peat	Tln-1312	9320 ± 75	8755–8331
3-85-54	2.0	Wood	Tln-1301	8040 ± 100	7300–6658
3-85-54	3.7	Wood	Tln-1297	9540 ± 190	9331–8321
3-85-2025	1.65	Wood	Tln-1292	10230 ± 95	10450–9463

(VSMOW) was adopted. GMWL – global meteoric water line–describes a linear relationship between the content of ^{2}H and ^{18}O in precipitation according to the following equation $\delta^{2}H = 8\delta^{18}O + 10$. Enrichment of deuterium compared to the heavy oxygen (called deuterium excess referred to d_{exc}) occurs in no equilibrium evaporation and condensation, which allows estimating the degree of no equilibrium systems (Vasil'chuk and Kotlyakov, 2000).

Isotopic analyses made in the isotope laboratory of the Institute of Geology of Estonia (R.A. Vaikmäe) using mass-spectrometer Finnigan Delta-E (Vaikmäe and Vasil'chuk, 1991) and in the isotope laboratory of the Alfred Wegener Institute for Polar and Marine Research Potsdam in Germany (H.Meyer) using mass-spectrometer Finnigan MAT Delta-S (Tables 2 and 3). Measurement errors of hydrogen and oxygen are 0.8‰ and 0.10‰, respectively (Meyer et al., 2000).

Several control samples were analyzed by Yu.Vasil'chuk, N.Budantseva and Ju.Chizhova using a mass-spectrometer Delta-V in isotope laboratory at the Department of Geography, Moscow State University in May and September 2009.

Sampling from ice wedge #7 was performed by step of 0.2 m in vertical and by step of 0.3 m in the horizontal direction. The sampling resolution is 1 m for ice wedge #10 due to non-frontal cut and large size (more than 4 m width) of the wedge. Pure ice without impurities was placed in plastic bags and labeled. Ice water after thawing was transfused into glass bottles of 50 mL. Wedges and segregated ice, water from the river and lake, located near the investigated ice wedges; rainwater and snow were sampled for isotopic analysis.

Table 2
Stable oxygen isotopes composition (δ^{18}O) in ice wedges and segregated (segr.) ices in the 6–8 m Chara River terrace, water from Chara River, rain and snow. Sampling was done in 1985 and 1988. Analytical determinations were done in the isotope laboratory at the Estonian Institute of Geology using mass-spectrometer Finnigan Delta-E.

Sample ID	Depth (m)	Ice	δ^{18}O (‰)	Sample ID	Depth (m)	Ice	δ^{18}O (‰)
Ice wedge 1, δ^{18}O mean value −23.0‰							
353-YuV/4	1.2	Ice wedge	−23.3	353-YuV/10	2.7	Ice wedge	−24.5
353-YuV/5	1.5	Ice wedge	−23.5	353-YuV/11	3.0	Ice wedge	−23.9
353-YuV/6	1.1	Ice wedge	−23.0	353-YuV/12	4.3	Ice wedge	−21.9
353-YuV/7	2.0	Ice wedge	−24.7	353-YuV/13	5.0	Ice wedge	−22.5
353-YuV/9	2.4	Ice wedge	−24.1				
Modern ice wedge, δ^{18}O mean value −21.55‰							
353-YuV/19	1.2	Modern ice wedge	−22.4	353-YuV/20	1.6	Modern ice wedge	−20.7
Ice wedge 2, δ^{18}O mean value −23.5‰							
353-YuV/23	0.7	Ice wedge	−24.5	353-YuV/25	1.2	Ice wedge	−23.8
353-YuV/24	2.5	Ice wedge	−22.2				
Buried ice wedge 3, δ^{18}O mean value −19.35‰							
353-YuV/16	5.2	Ice wedge	−20.9	353-YuV/17	5.4	Ice wedge	−17.8
Ice wedge 4, δ^{18}O mean value 23.0‰							
3-85-54/1	1.3–1.4	Ice wedge	−24.9	3-85-54/3	3.8–4.0	Ice wedge	−22.0
3-85-54/2	2.1–2.2	Ice wedge	−25.3	3-85-54/4	5.0–5.4	Ice wedge	−19.8
Ice wedge 5, δ^{18}O mean value −25.1‰							
3-85-5-15/1	1.5	Ice wedge	−24.6	3-85-5-15/3	3.4–3.5	Ice wedge	−25.7
3-85-5-15/2	2.4–2.5	Ice wedge	−25.0				
Ice wedge 6, δ^{18}O mean value −21.2‰							
3-85-36/1	1.4–1.6	Ice wedge	−21.2				
Ice wedge 12 in Rzhavy Creek valley, δ^{18}O mean value −26.37‰							
2094-85-1	2.7–2.8	Ice wedge	−23.9	2094-85-3	2.4–2.6	Ice wedge	−30.0
2094-85-2	2.7–2.8	Ice wedge	−25.2				
Segregated ice lenses near ice wedge 1, δ^{18}O mean value −16.08‰							
353-YuV/19	1.2	Segr. ice from sandy loam	−16.1	353-YuV/18	1.5	Segr. ice from peat	−14.3
353-YuV/15	4.7	Segr. ice from sand	−14.4	353-YuV/26	1.8	Segr. ice from sandy loam	−19.5
Rain, snow, river water, δ^{18}O mean value −23.33‰							
353-YuV/21	–	Rain, August 1988	−15.8	353-YuV/22	–	Chara River water, August 1988	−19.5
3-85-1	–	Snow, 1985, Udokan	−39.9	3-85-33/1	–	Chara River water, July 1987	−18.1

Table 3
Stable oxygen isotopes composition (δ^{18}O), hydrogen (δ^{2}H) and deuterium excess values (d_{exc}) in ice wedges and segregated (segr.) ice in the 6–8 m Chara River terrace and in the saddle of Udokan ridge near Uschelisty creek. Sampling was done in 2006–2009. Analytical determinations were done in the isotope laboratory of the Institute for Polar and Marine Research Alfred Wegener, Potsdam (Germany) using mass-spectrometer Finnigan MAT Delta-S.

Sample ID	Depth (m)	Type of ice	δ^{18}O (‰)	δ^{2}H (‰)	d_{exc} (‰)	Sample ID	Depth (m)	Type of ice	δ^{18}O (‰)	δ^{2}H (‰)	d_{exc} (‰)
Ice wedge 7, mean values of δ^{18}O 21.24‰, δ^{2}H 174.85‰											
JuS-Chara/6-26	1.5	Ice wedge	−20.24	−163.1	−1.2	JuS-Chara/6-9	1.9	Ice wedge	−20.88	−173.7	−6.7
JuS-Chara/6-1	1.5	Ice wedge	−20.65	−171.1	−5.9	JuS-Chara/6-7	1.9	Ice wedge	−21.18	−175.1	−5.6
JuS-Chara/6-24	1.5	Ice wedge	−21.66	−173.2	0.1	JuS-Chara/6-10	1.9	Ice wedge	−22.71	−183.6	−1.9
JuS-Chara/6-25	1.5	Ice wedge	−20.05	−167.3	−6.9	JuS-Chara/6-28	2.1	Ice wedge	−21.86	−175.7	−0.8
JuS-Chara/6-22	1.7	Ice wedge	−20.74	−166.2	−0.3	JuS-Chara/6-20	2.1	Ice wedge	−21.21	−177.4	−7.8
JuS-Chara/6-5	1.7	Ice wedge	−21.63	−178.1	−5.1	JuS-Chara/6-19	2.1	Ice wedge	−19.34	−171.0	−16.3
JuS-Chara/6-11	1.7	Ice wedge	−20.61	−180.5	−15.7	JuS-Chara/6-8	2.3	Ice wedge	−21.36	−177.6	−6.7
JuS-Chara/6-2	2.5	Ice wedge	−22.21	−179.0	−1.4	JuS-Chara/6-27	2.3	Ice wedge	−23.53	−185.0	3.2
Segregated ice, mean values of δ^{18}O −15.66‰, δ^{2}H −130.35‰											
JuS-Chara/6-3	1.2	Segr. ice (sandy loam)	−15.77	−133.0	−6.9	JuS–Chara/7–29	1.2	Segregated ice	−15.54	−127.7	−3.4
Ice wedge 8											
JuS-Chara/6-21	1.4	Ice wedge	−17.16	−138.5	−1.2						
Ice wedge 9, mean values of δ^{18}O −23.39‰, δ^{2}H −183.95‰											
JuS/8-1	2.5	Ice wedge	−23.71	−187.6	2.1	JuS/8-2	2.5	Ice wedge	−23.06	−180.3	4.2
Ice wedge 1, mean values of δ^{18}O −22.74‰, δ^{2}H −180.50‰											
JuS-Chara/7-25	1.7	Ice wedge	−23.92	−188.8	2.6	JuS-Chara/7-15	1	Ice wedge	−22.62	−177.1	3.9
JuS-Chara/7-27	1.7	Ice wedge	−21.67	−175.6	−2.2						
Ice wedge 11, Udokan ridge near Uschelisty creek											
JuS-Chara/7-2	0.10	Segr. ice (peat)	−15.27	−117.9	4.3	JuS-Chara/7-3	0.45	Ice wedge	−22.3	−169.9	8.5
Blister ice on the west part of Chara Sands, mean values of δ^{18}O −15.25‰, δ^{2}H −124.05‰											
JuS-Chara/6-12	0.5	Blister ice	−15.1	−124.4	−3.9	JuS-Chara/6-13	0.4	Blister ice	−15.4	−123.7	−0.6
Icing mound, Nerungri, January mean values of δ^{18}O −20.90‰, δ^{2}H −159.28‰											
YuS-Ner/7-2	–	Icing	−19.2	−151.7	1.9	YuS-Ner/7-7	–	Icing	−23.2	−175	10.6
YuS-Ner/7-3	–	Icing	−19.6	−151	5.8	YuS-Ner/7-9	–	Icing	−22.8	−169.5	12.9
YuS-Ner/7-8	–	Icing	−19.7	−149.2	8.4	YuS-Ner/7-10	–	Snow abo-we icing	−39.3	−297.3	17.1
River icing, mean values of δ^{18}O −18.45‰, δ^{2}H −148.4‰											
YuS-Ner/7-3		Icing, Berkakit river	−19.5	−156.8	−0.8	YuS-Ner/7-1	Icing, Nerungra river		−17.4	−140	−0.8
Gorbylakh, segregated ice of palsa, mean values of δ^{18}O −10.15‰, δ^{2}H −95.55‰											
YuS-Gor/6-5	0.8	Ice lenses	−12.3	−103.9	−5.7	YuS-Gor/6-1	1.2	Ice lenses	−8	−87.2	−23.2
River water, mean values of δ^{18}O −18.77‰, δ^{2}H −143.95‰; October snow, mean values of δ^{18}O −39.30‰, δ^{2}H − 286.10‰											
JuS-Chara/7-28	–	Chara River, water	−18.28	−139.5	6.7	JuS-Chara/7-4	–	Udokan Lake, water	−13.27	−108.6	−2.4
JuS-Chara/8-1	–	Snow, 15.10.08	−36.17	−264.3	25	JuS-Chara/8-2	–	Snow, 02.10.08	−42.42	−307.9	31.4
JuS -Ner/7-2	–	Nerungra River water	−20.9	−162	5.2	JuS -Ner/7-6	–	Chulman River water	−18.1	−138.7	6.1
JuS -Ner/7-4	–	Berkakit River water	−17.8	−135.6	6.8						

4. Results

4.1. Cryostratigraphy of deposits with ice wedges

The section of fine- and medium-grained sand with gravel and pebble layers of up to 0.5 m was excavated in one of the parts of the exposure (Fig. 5). Here ice wedges up to 7 m high were detected. Large ice wedges #1 and #3 occur in sandy sediments with gravel layers at the depth of 1 m and 5 m, respectively (Fig. 5b). Ice wedge #2 was buried and preserved in the flood plain deposits under the peat at the depth of 3 m. The modern ice wedge was discovered in peat in another part of the exposure.

Layers are exposed in another part of this exposure (Fig. 5a) as follows (described from the top):

- 0–1.8 m – ice-poor sandy loam and loam with horizontal wavy stratification.
- 1.8–5.0 m – peat layers interbedded with fine-grained sand, sandy loam and loam with horizontal stratification. Ice wedges #5 and #6 occur in these sediments. Thick layers of peat are traced to the depth of 2.5 m.
- 5.0–6.7 m – gray sand from medium to coarse with fine gravel and single inclusions of angular quartz clasts up to 1–2 cm. Diagonal bedding is traced in sand mostly. Ice wedge #4 occurs at the depth of 1.4 m from the top of this lager.

The third part of this exposure consists of sand of 5–6 m thick with gravel inclusions, overlain by ice-reach dark-brown 1.5 m peat layer of low degree of decomposition (Figs. 6 and 7). Ice wedges #7, #8, #9 and #10 occur here at different depths.

Ice wedge #7 is covered by frozen peaty sandy loam from the depth of 0.7 m with horizontal ice lenses 0.3–7 cm thick. The spacing between ice lenses increases from the top to the bottom from 1 to 10 cm. Micro-lenticular (French and Shur, 2010) cryostructure with vertical ice veins was detected between these ice lenses. Ice is transparent with vertical air bubbles.

Vertical extent of the ice wedge #7 is 5 m, and occurs top at the depth of 1.5 m. Ice wedge consists of two parts: a "head" 2 m wide and 1 m high, and a "tail" 0.2–0.7 m wide and 4 m high. Ice of "head" by milky color with vertically layered structure and the inclusion of air bubbles. Ice of wedge "tail" has dirty milk color with fuzzy structure close to fine-grained. Side contacts of wedges are smooth. "Tail" of ice wedge is narrow and ends in a layer of peat 0.3 m thick. The soil is lowland sedge-hypnum peat with the decomposition degree of 20%–35% and ash content of dry substance is 24.86%. The peat composition includes: *Carex rubra Levl. Et Vaniot*. 25%, *Calamagrostis* 25%, *Calliergon stramineum* + *Calliergon* sp. 40% and 10% of grass (analyses by O.N. Uspenskaya).

Ice wedge #8 also occurs in the peat close to the ice wedge #7 (Fig. 6). The "head" of ice wedge #8 (Fig. 7) lies at the depth of 1.3 m and is covered by sandy loam with horizontal ice lenses. The thickness of ice lenses is up to 2.5 mm 20 cm-wide ice "shoulders" occur at the depth of 1.65 m. Wedge ice has a vertical foliation. The total height of ice wedge #8 is 1 m.

Ice wedge #9 is located to the left from ice wedge #7. It lies at the depth of 2 m in the sands interbedded with gravel, covered by peat (Fig. 6). Ice is wedge-shaped, its width and height are 2 m. Thick ice wedge #10 is found at the depth of 0.8 m (see Fig. 6). "Head" of wedge lies in 1.5-m-thick peat, rest of wedge penetrates into the underlying sand deposits. Width of this ice wedge in non-frontal section is 7 m, although its true width is likely to be about 1–1.5 m.

Ice wedges are developing actively at intermountain saddle near Uschelisty Creek on the Udokan ridge at 1600–1700 m.a.s.l. Polygonal patterned ground is clearly defined on the territory. Ponds located on the saddle are 4 m × 5 m in size and approximately 0.3 m deep. Vegetation is represented by dwarf birch, rhododendron, wild rosemary and moss. Ice wedge #11 was hand drilled on polygonal ridge. Ice wedge was encountered at the depth

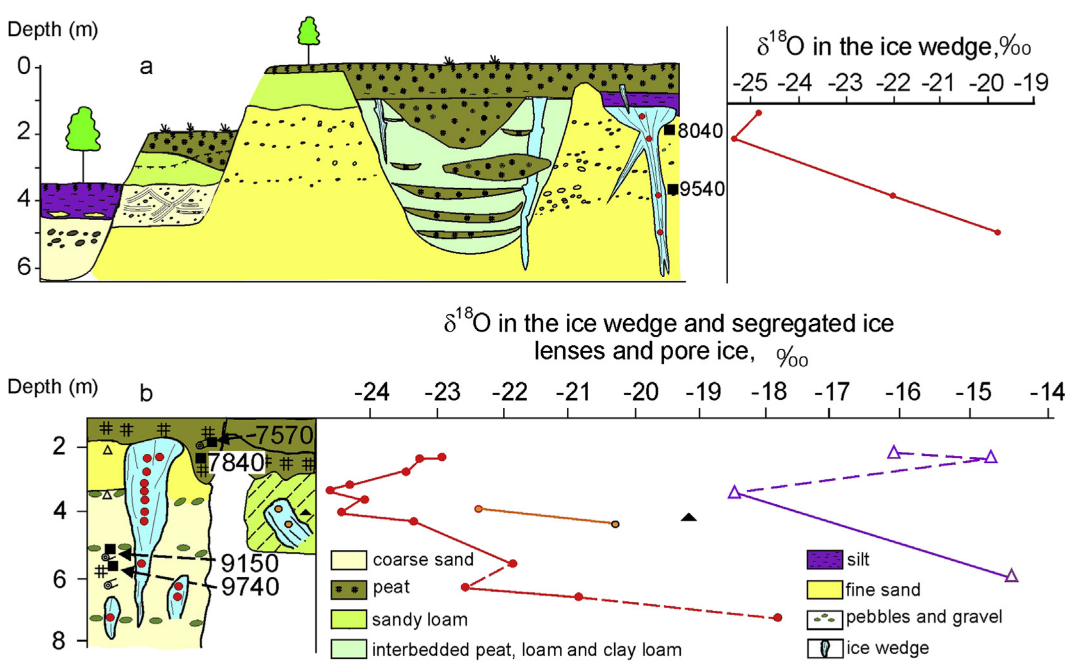

Figure 5. Radiocarbon age of organic sediments and $\delta^{18}O$ values in ice wedges of the 6–8 m Chara River terrace: a – ice wedge #4, 5 and 6; b – ice wedge #1, ice wedge #2 under peat and buried ice wedge #3.

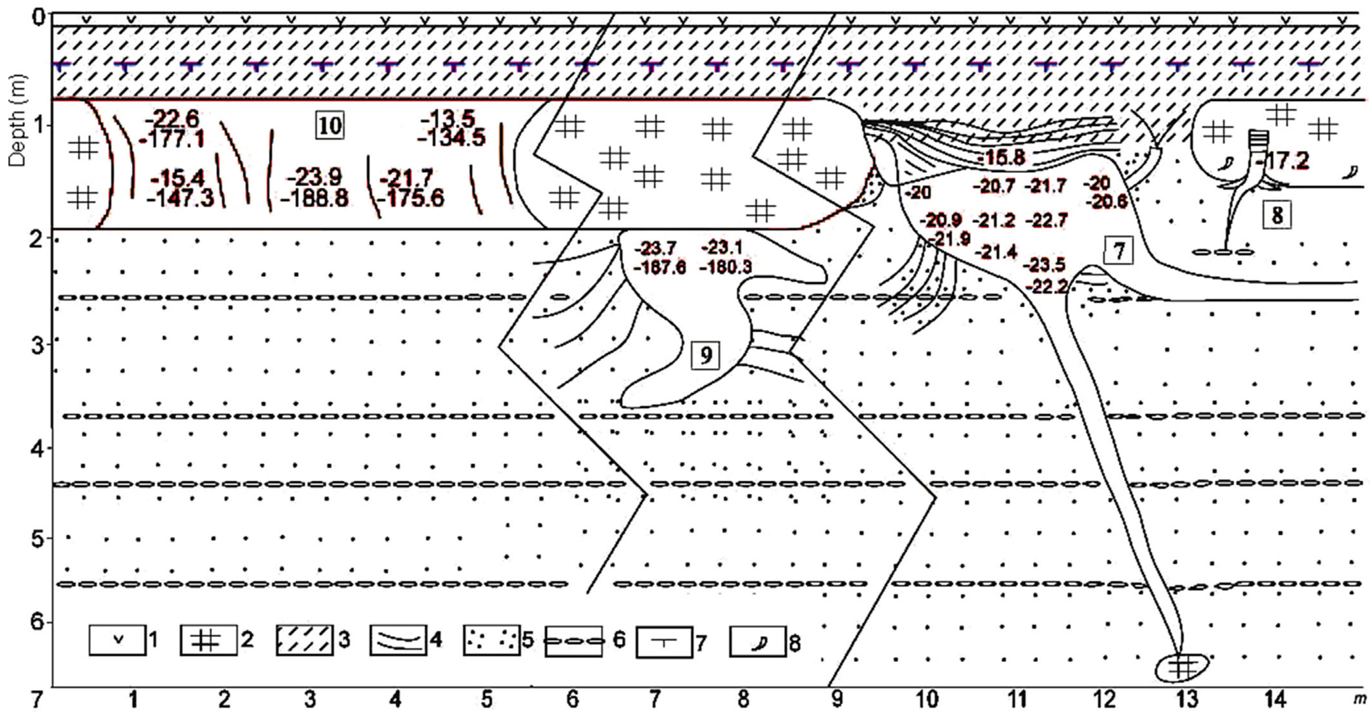

Figure 6. Ice wedges #7, #8, #9 and #10 in the "Belyi Kluch" exposure of the 6–8-m terrace of the Chara River: 1 – vegetation cover; 2 – peat; 3 – peaty sandy loam; 4 – ice lenses; 5 – cross–bedded sand interbedded with gravel; 6 – gravel; 7 – seasonal thawing layer; 8 – inclusion of wood. Note: The numbers denote the isotopic composition of ice wedges in ‰ (upper – on $\delta^{18}O$ and lower – on δ^2H). Description and sampling performed in 2006–2008.

of 0.4 m and covered by frozen well-decomposed dark-brown peat. Virtually all of the studied ice wedges are syngenetic.

4.2. Radiocarbon dating of deposits containing ice wedges

All 19 ^{14}C ages refer to a range of 10 to 7.5 ka BP (Vasil'chuk and Vasil'chuk, 1995; Vasil'chuk et al., 2006). This period coincides with the first half of the Holocene climatic optimum for these regions of Siberia (Vasil'chuk, 1992, 2006, 2013). Absence of gaps in the ages of the wood shows that woody vegetation grew throughout the period of the terrace deposits accumulation. Though re-deposition of organic material in the river alluvium is quite possible under the intermountain conditions, radiocarbon ages show no significant re-deposition of ancient organic material in the 8-m terrace. An important indicator of this is increase in the ^{14}C age with the depth (Fig. 8).

There are no any age inversions between ^{14}C ages of the wood and surrounding peat (Table 1). This means that both the peat and wood formed simultaneously, and in this case, re-working is unlikely.

4.3. Palynological analysis of deposits containing ice wedges

Lower sand layer is characterized by predominance of *Pinus sylvestris* pollen and *Selaginella* spores. Maximum percentage of *Larix* (larch) pollen is replaced by a maximum of *Pinus sylvestris* and *Betula* pollen during overall dominance of AP (arboreal pollen) (64%–70%) at the depth from 6.0–5.5 m up to 4.6 m. *Sphagnum* dominates among the spores. Maximum of *Artemisia* pollen coincides with local maximum of *Betula* content that is likely to respond to the arid conditions.

The ratio of the main components is different in the middle part of the section in clays and loams. Spores of mosses and ferns are dominant. A maximum of Caryophyllaceae pollen occurs at the depth of 4.3 m, which may indicate the polygonal structures development and possible decrease in summer temperatures and beginning of development of polygonal mires mire development. Wood pollen content is reduced to 7%–38% and participation of Bryales and Polypodiaceae (58%–90%) is increased at the depth of 4.3–3.4 m. Increase in *Betula* sect. *Nanae* (36%–40%), shrub and tree species of *Salix* characterizes the pollen spectra of this interval. The pollen of *Artemisia* and other Compositae dominates among grass; pollen of Chenopodiaceae and *Epilobium* is found. Since local components of pollen spectra were absent, deposition occurred in conditions of significant deterioration in the terms of vegetation and abrupt environmental changes and summer temperatures.

Increase in the AP pollen percentages together with the dominance of *Pinus sylvestris* pollen is marked at 0.1–2.8 m. The peak of the *Betula* sect. *Nanae*, which is replaced with a maximum of *Betula* and *Alnus*, occurred at the depth of 1.5 m. The Ericaceae together with Chenopodiaceae and *Artemisia* dominates among grass pollen. Pollen of *Ephedra* and *Epilobium* were also found. *Sphagnum* spores prevail at upper part of the terrace sediments (Klimovsky and Vasilyeva, 1967). This indicates the completion of the mire development process and changing soil nutrition with atmospheric.

4.4. Isotopic analysis of ice wedges and lenses of segregated ice

Values of $\delta^{18}O$ of major ice wedge #1 vary from −24.7‰ to −21.9‰ (Fig. 5b). In ice wedge #4 values of $\delta^{18}O$ range from −25.3‰ to −19.8‰. In ice wedge #5 $\delta^{18}O$ varies from −25.7‰ to −24.6‰ (Fig. 5a). In ice wedge #7 $\delta^{18}O$ ranges from −19.34‰ to −23.53‰ (Fig. 9), on average −21.4‰, while δ^2H values range from −163.1‰ to −185‰ (Fig. 10), averaging −174.9‰.

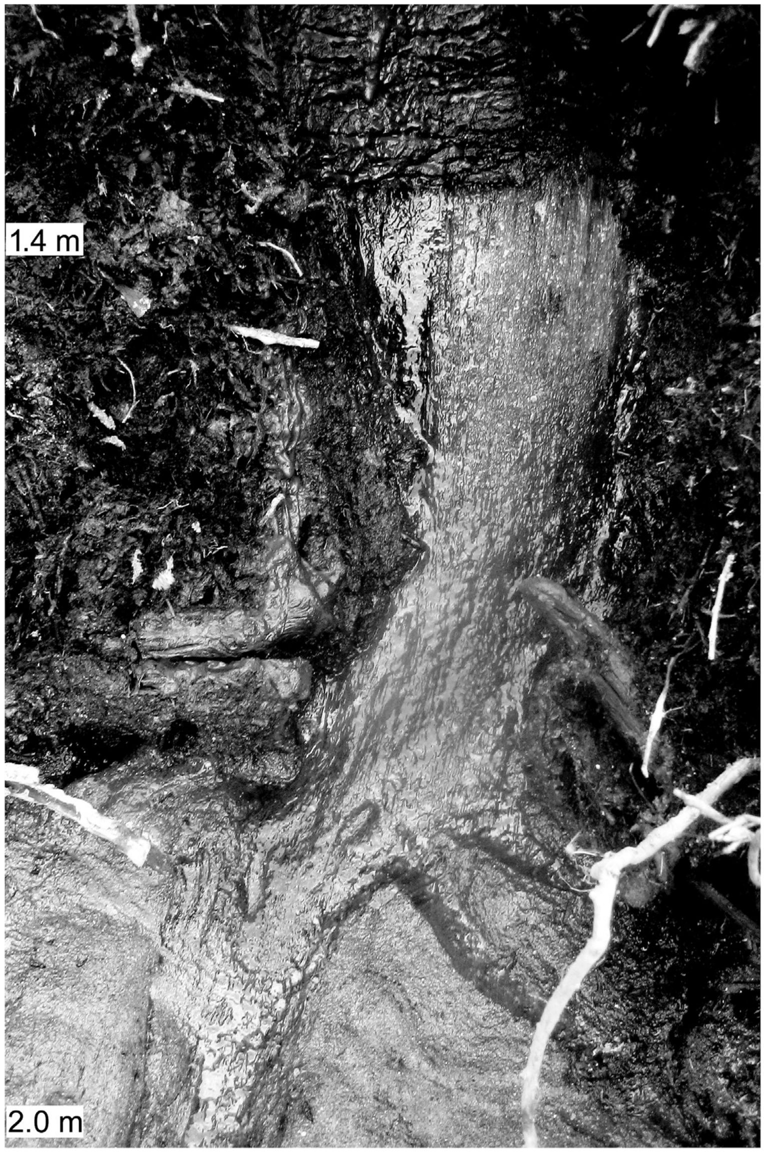

Figure 7. Buried ice wedge #8 with ice shoulders in peat at the site “Belyi Kluch”. Photo by Ju.V.Stanilovskaya, 2006.

In ice wedge #9 δ^{18}O averages −23.38‰, δ^2H is −183.4‰. The isotopic composition of ice wedge #10 for δ^{18}O varies from −21.7‰ to −23.9‰, on average −22.7‰; for δ^2H varies from −188.8‰ to −175.6‰, the average value is −180.5‰ (Fig. 6). In the buried ice wedge #8 δ^{18}O = −17.2‰, δ^2H = −138.5‰. δ^{18}O of modern ice wedge varies from −22.4‰ to −20.7‰, averaging −21.5‰. The isotopic composition of ice wedge #11 on the saddle of the Udokan Ridge is −22.30‰ for δ^{18}O and −169.9‰ for δ^2H, water of the adjacent lake is −13.27‰ for δ^{18}O and −108.6‰ for δ^2H. The isotopic composition of thin ice lenses in sand and gravel is heavier (δ^{18}O varies from −18.5‰ to −14.4‰). At the same time the ice in the sandy loam underlying bog peat is isotopically lighter (δ^{18}O = −19.5‰). Values of δ^{18}O in the ice lenses in sand overlying the ice wedge #1 and #7 constitute −16.1‰ and −15.8‰, respectively. δ^{18}O in the ice lenses in peat overlying ice wedge #11 is −15.27‰ and δ^2H is −117.9‰.

The isotope composition of the Chara River water varies from −18.2‰ to −19.5‰ for δ^{18}O and is −139.5‰ for δ^2H. δ^{18}O value of a fresh snow (2 and 15 October, 2008) in the Chara River valley varies from −36.17‰ to −42.42‰, and δ^2H from −264.3‰ to −307.9‰.

Range and mean values of δ^{18}O, δ^2H and d_{exc} in wedges and ice lenses are presented in Table 3. Years of sampling and analysis are shown as the definitions were performed in different laboratories, and isotopic measurements in connection with the use of different standards may differ slightly from each other. The differences in δ^{18}O values are 0.4‰–0.2‰ as shown by test measurements of the same samples made in different laboratories. Average values of oxygen isotopic composition of samples obtained in different years are:

- a large ice wedges in the Chara River terrace for δ^{18}O of −23.5‰ (1988), −24‰ (1985), −21.43 ‰ (2006), −23.38‰ (2008) for δ^2H of −175‰ (2006), −183.4‰ (2008);
- in ice wedge on the Udokan ridge saddle −22.30‰ for δ^{18}O and δ^2H of −169.9‰ (2007);

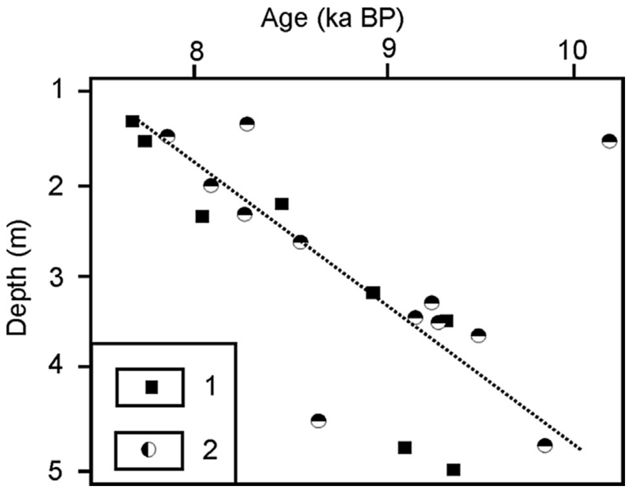

Figure 8. Radiocarbon age of organic sediments adjacent to ice wedges exposed in the 6- to 8-m-high Chara River terrace with depth (from Vasil'chuk et al., 2006). Samples: 1 – wood; 2 – peat.

- in structure ice on $\delta^{18}O$ of $-16.1‰$ (1985), $\delta^{18}O$ of $-15.8‰$ and $\delta^{2}H$ of $-133‰$ (2006), $\delta^{18}O$ of $-15.27‰$ and $\delta^{2}H$ of $-117.9‰$ (2007);
- in buried ice wedges $\delta^{18}O$ of $-17.2‰$ and $\delta^{2}H$ of $-138.5‰$ (2006);
- in modern ice wedge $\delta^{18}O$ of $-21.5‰$ (1988);
- in modern blister ice $\delta^{18}O$ of $-15.2‰$ and $\delta^{2}H$ of $-124‰$ (1988);
- in the Chara River water for $\delta^{18}O$ of $-18.6‰$ and $\delta^{2}H$ of $-139.5‰$ (1985, 1988, 2007);
- in the water of the lake on the Udokan ridge saddle near creek Uschelisty $-13.27‰$ for $\delta^{18}O$ and $\delta^{2}H$ of $-108.6‰$ (2007);
- in autumn snow $-39.29‰$ for $\delta^{18}O$ and $-286.1‰$ for $\delta^{2}H$ (2008);
- in rainwater $-16.69‰$ for $\delta^{18}O$ (2009).

4.5. Winter temperatures, 10–7.5 ka BP

The average January temperature and average winter temperature during ice wedge formation calculated by using the equations (Vasil'chuk, 1992):

$$t_{jan} = 1.5\delta^{18}O\ (\pm 3\ ^\circ C),\ t_{winter} = \delta^{18}O_{wedge}\ (\pm 2\ ^\circ C)$$

Judging by the isotopic data, average winter temperature in the Chara Basin in the period from 7.5 to 10 thousand years ago, ranged from −25 to − 21 °C. But the most of the time temperature was −23 °C, i.e. was close to recent or 2–3 °C below. The average January temperature could reach −37, −38 °C in the most severe winters, i.e. was lower 3–4 °C than now. The freezing index ranged from −4350 to −5700 °C degree days and sometimes was close to modern ones, but mostly were lower than today.

If consider the evolution of the temperature regime of the large ice wedge #7 (Fig. 9) in "Belyi Kluch" site, we can conclude that frost cracking and ice wedge growth occurred at the floodplain surface. The "tail" of ice wedge #7 formed in more sever climatic conditions ($\delta^{18}O = -22.2‰$ and $-23.5‰$; Fig. 10) with an average January temperature of about −35 °C. Ice wedge continued to grow syngenetically in milder climate ($\delta^{18}O = -20‰$ to $-20.7‰$) with an average January temperature of about −31 °C (the mean January temperature in the Chara meteorological station for 1939–2004 is −33 °C). It can be concluded that the temperature regime in which the formation of ice wedge #7 occurred was close to recent climatic conditions or average January temperatures were lower by 1–2 °C.

Figure 9. Sampling points of ice wedge #7 on the "Belyi Kluch". Photo by Ju.V.Stanilovskaya.

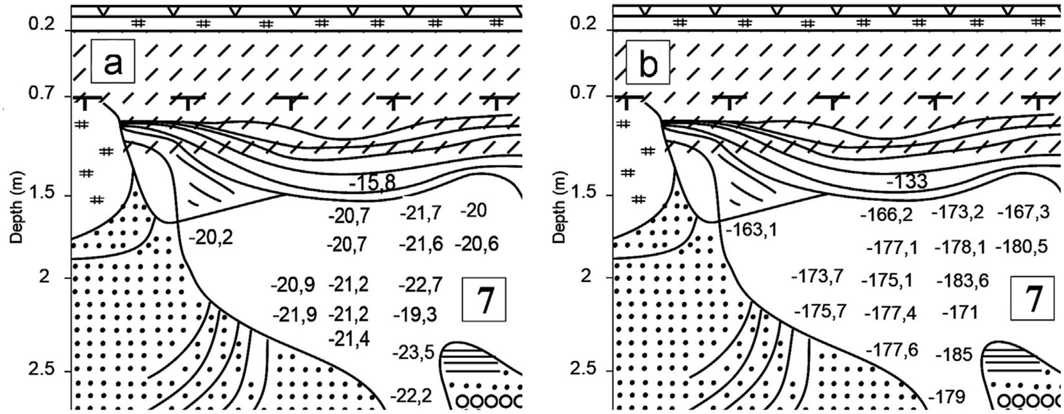

Figure 10. The values of $\delta^{18}O$ (a) and δD (b) in ice wedge #7. Symbols refer to Fig. 6.

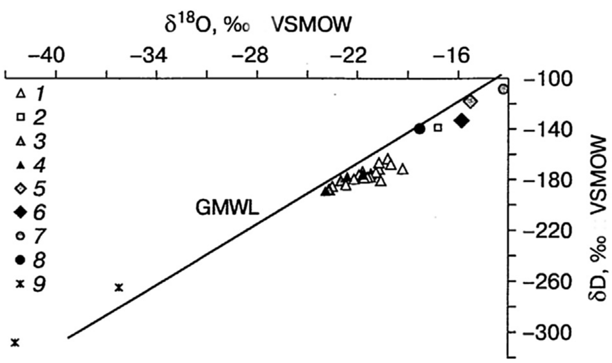

Figure 11. Isotopic compositions of ice wedges, lenses of segregated ice, river and lake water of the Chara Basin. VSMOW – Vienna standard mean ocean water, GMWL – global meteoric water line. Sampling was performed in 2006–2008. 1 – Belyi Kluch 1; 2 – Belyi Kluch 2; 3, 4 – ice lenses in the sand; 5 – ice lenses in the peat (Udokan site); 6 – Chara River water; 7 – small lake water (Udokan); 8 – rain 1988; 9 – snow.

Stable isotope analysis of ground ice from a deep borehole in permafrost in the Kunlun Mountain Pass (KLM) on the Qinghai-Tibet Plateau, China, was carried out to assess the water source and origin of the ground ice (Yang et al., 2016). According to this study isotope contents of segregated ground ice from KLM vary within narrower ranges than those of modern precipitation and surface waters: it increased gradually with depth from −11.9‰ to −8.7‰ for $\delta^{18}O$ and from −93.5‰ to −73.2‰ for δ^2H; d_{exc} values gradually decreased from 4.94‰ to −3.8‰ Using the negative slope between d_{exc} and δ^2H authors attributed ground-ice formation to the closed system.

4.6. Summer temperatures and vegetation, 10–7.5 ka BP

Judging by the ^{14}C dating, sediments, synchronous to syngenetic ice-wedge formation accumulated in the range of 10–7.5 ka BP, i.e. less than three thousand years. The short duration of periods of summer temperature oscillations led to different responses of vegetation components. Herbaceous plants react to the short-term change in temperature by the plant community's composition; woody vegetation could not reflect temperature changes at this scale. Taking into account short-term climatic fluctuations, primarily it's possible to fix the fluctuations in NAP (non arboreal pollen). Note that the total thawing index ranged from 1400 to 1600 °C degree days in the last 70 years.

Thin lenses of autochthonous peat were dated 9320 ± 75, 9150 ± 80, 8980 ± 80, 8875 ± 65, 8035 ± 55, 7570 ± 250 ^{14}C years BP (Vasil'chuk et al., 2006). This means that conditions for the autochthonous peat accumulation occurred during the formation of deposits with ice wedges. Autochthoneity of the peat is confirmed by the coincidence of peat and wood dates. In this case, the rate of deposit accumulation during subaqueous phase is approximately 1 m in 400 years or 2.5 mm/yr.

Three pollen phases were distinguished by analyzing of pollen spectra based on changing pollen taxa composition and abundances. The first one corresponds to the 2-m of bottom sand layer. It is characterized by highest abundance of pine, birch, spruce and larch. Conditions during accumulation of the sand were the most favorable and characterized by relatively high temperatures and humidity. It is a phase of larch forests and pine and birch forests with spruce and dwarf birch. According to the method of total summer temperature (A.Vasil'chuk, 2007), the thawing index during the first period at the initial phase of the Holocene Optimum was estimated as 1600–1800 °C degree days, i.e. it was slightly higher than today's value (up to 1800 °C degree days) or close to it.

The second pollen phase corresponds to the prevalence of fens and birch-pine woodlands with ferns at the final stage of the sand layer accumulation. During this time, a decrease in the thawing index up to 1300 °C degree-days was possible, which is approximately 300 °C degree-days less than modern values. Increase of wood pollen during the third pollen phase indicates expansion of birch-pine forests with larch and spruce. This is evidenced by the occurrence of Ericaceae and forest species of Lycopodiopsida in the spectra. The thawing index was close to the modern (1550–1600 °C degree-days).

The pollen spectra at depths of 4.3, 2.7 and 1.5 m reflect the extension of polygonal landscapes and ice-wedge growth. Indicators of the polygonal tundra are the domination of *Sphagnum* and Bryales in these spectra with *Betula* sect. *Nanae*, Caryophyllaceae, *Artemisia* (A.Vasil'chuk, 2016). Study of ice-wedge mire in Herschel Island (Fritz et al., 2016) shows that peaks in *Salix* and Brassicaceae pollen occur at the stage of mire development and ice-wedge cracking. A slight increase in Cyperaceae and a concomitant decrease in Poaceae is observed, reflecting the shift from a regionally derived pollen signal toward representation of local wetland vegetation. At the pollen plot of the permafrost core from Herschel Island minor peaks in Caryophillaceae and Rosaceae is observed also.

5. Discussion

5.1. Syngenetic permafrost with ice wedges of the Holocene age in the Chara region and adjacent areas

The obtained results allow concluding that syngenetic permafrost formed in northern Transbaikalia throughout the Holocene, including the Holocene Optimum. Here we discuss main features of the syngenetic permafrost with ice wedges in the Chara region and adjacent areas.

Ice wedge in Holocene deposits of Central Yakutia was investigated by Popp et al. (2006) in the coastal outcrops of the Tumara River. Wedge is situated in a thick layer of peat and underlying river sand and gravelly deposits. The width and vertical extent of the wedge are about 0.5 and 1.8 m, respectively. Organic remains in sand deposits under the wedge are radiocarbon dated to 8539 ± 44 years BP (KIA-19144) at the depth of about 2.5 m. The isotopic composition of the ice wedge, formed in the Tumara River valley during the first half of the Holocene optimum, in similar facies conditions as ice wedges in the Chara River terrace, is equal to $\delta^{18}O$ of −25.94‰ and $\delta^{2}H$ of −199.4‰, the average value is d_{exc} of 8.2‰. These data are similar to the isotopic values of ice wedges on the Chara River terrace and indicate that ice wedges were actively growing in sandy-gravelly sediments in central Yakutia and in northern Transbaikalia during the Holocene optimum.

5.2. Climate, vegetation, and ice-wedge formation, 10–7.5 ka BP

Permafrost was greatly affected by the warming and wetting climate in northeastern China 10–7.5 ka BP. It had a significant presence in the northern part with at about 52°N. During the Early Holocene, dark needle-leaved forests gradually moved northwards and eventually out of the southern part of northeast China (Feng et al., 2013; Sun and Feng, 2013; Tian et al., 2017); as they climbed upwards into mountains, birch forests prevailed below. However, in comparison with today, spruce and fir were still more extensively distributed in the northern part, as suggested by the presence of spruce and fir pollens (Jin et al., 2016). Pollen analysis of the Huola section in NE China (Zhao et al., 2016) also indicates that vegetation experienced a transformation from early-mid Holocene warm-cold mixed vegetation to late Holocene cold-temperate vegetation. From 9100 to 6000 cal yr BP, it was warmer and wetter than at present, developing *Corylus, Carpinus, Pinus, Picea, Betula* and *Larix*-dominated forests. Two cooling events at 6000–5000 and 3500–2500 cal yr BP led to a decrease in *Corylus*, *Carpinus* and other thermophilic vegetation, whereas cold temperate forests composed of *Larix* and *Betula* expanded at that time. The biome maps of northern part of central Asia, show that there is little evidence of an expansion of dry-land biomes, which might be expected with heightened aridity for 7 ka cal BP (Binney et al., 2017). In the northern Da Xing'anling Mountains ice wedges at Wuma (120°45′E, 52°58′N) have been preserved continuously until the present, i.e. permafrost had not completely backed out of northeast China.

Locality of Holocene ice wedges is Merzlyi Yar outcrop situated in the eastern part of Tuva Republic on the right bank of the Bolshoi Yenisei River within the Todzha Basin (52°31′48″N, 95°21′46″E). According to the ^{14}C dates of the host sediments from 3750 to 11350 BP ice wedges formed during the Holocene (Vasil'chuk et al., 2002). Reconstruction of the quantitative characteristics of temperature has been done by using isotopic data. The $\delta^{18}O$ values vary from −22.58‰ to −25.25‰, and $\delta^{2}H$ from −191‰ to −203.6‰. The difference between deuterium and ^{18}O values, coincidental with the Global Meteoric Water Line (Fig. 11), may be caused by continental climate and the great distance from the moisture source. The isotopic data also demonstrate that the mean winter temperature fluctuations during the period of ice wedge formation did not exceed 2–3 °C, and in January no more than 3–5 °C. This means that winters during the Holocene optimum were no milder than present winters with mean January temperatures between −27 and −31 °C (Vasil'chuk et al., 2002). Pollen spectra from sediment aged 10–7.5 ka BP are characterized by abundance of *Pinus sibirica* and *Picea obovata* throughout the core (up to 60%); *Pinus sylvestris* occur with about 15%–20% (Arzhannikov et al., 2010).

5.3. Ice-wedge occurrence in gravelly and pebbly sediments

Ice wedges are quite rare in gravel and pebble sediment. It is believed that in relatively warm environments they develop mainly in organic and fine-grained mineral soils. However, in paleo permafrost areas there are many ice wedge pseudomorphs in gravel and pebbles (Johnsson, 1982; Murton and Kolstrup, 2003). However, the ice wedges in these sediments are rare, and usually the ice wedges are confined to the valleys of mountain rivers. One of the first ice wedges in gravels was described by Heginbottom and Tarnocai at "Boot Gully" borrow pit (Supplementary Fig. S3) (French and Heginbottom, 1983). In Siberia in the valley of the Biryusa and Issiley Rivers ice wedges in the gravel were described by Osadchy (1982). We described the ice wedges in 20 m exposure with 3 layers of gravel of up to 0.5 m. In the valley of the Chara River large ice wedges dissect the gravel horizons, and there are buried small veins under gravel layers.

Isotope composition of the Holocene ice wedges in the north Da Hinggan Mountains and stretches along the Yitulihe River is comparable with that in Chara (Yang et al., 2015). With ^{14}C age not older than 5 ka BP, these ice wedges are comparable with final stage of ice-wedge formation in Chara outcrops. The $\delta^{18}O$ values are characterized by small variation (3.1‰) from −20.9‰ to −17.8‰ throughout the profile. The weighted mean value for the 16 samples is −18.8‰ for $\delta^{18}O$. The maximum and minimum values differ from this value by 1.0‰ and −2.1‰, respectively. The mean value of $\delta^{2}H$ is −151.0‰, ranging from −171.0‰ to −141.7‰. The stable isotopes plot reveals three periods of temperature fluctuations detected at approximately 2.8, 2.3 and 1.9 ka BP.

6. Conclusions

Detailed testing of ice wedges from different parts of the exposure, radiocarbon, pollen and isotopic study allowed to specify the time and conditions of ice-wedge formation:

(1) Syngenetic ice wedges up to 7 m high were actively formed during the Holocene (dated 10–7.5 ka BP) in sands interbedded with pebbles and gravel of the Chara River valley (not in the Late Pleistocene, as had been stated in the previous studies). It is proved by ^{14}C age of sediments and isotope composition of the ice wedges. Mean value of $\delta^{18}O$ is −23‰ and $\delta^{2}H$ −180‰. Comparison of the isotopic composition of Holocene and modern ice wedges showed that the $\delta^{18}O$ values of the Holocene were more negative by 1‰–3‰.

(2) Conversion of isotopic data to palaeotemperature showed that the average winter temperature of the cold stages of the Holocene optimum (10–7.5 ka BP) could be colder than today by 2–3 °C and average January temperature by 3–4 °C. The freezing index could drop to −5100, −5700 °C degree-days, i.e. it was even lower than the extremely cold modern winters by

300–600 °C degree-days. At warmer stages of Holocene climatic optimum winter temperatures were close to modern ones.

(3) Judging by the pollen spectra, the thawing index during 10–7.5 ka BP ranged from 1300 to 1800 °C degree-days, i.e. was slightly higher and sometimes lower than modern ones.

Acknowledgments

The authors express special appreciation to Dr. V. Zaytsev for assistance in the field work and submitted materials. We thank Dr. N. Budantseva, Dr. Ju. Chizhova, Dr. H. Meyer and Dr. R. Vaikmäe for stable isotope analyzes. We are particularly grateful to Dr. M. Kanevskiy and one anonymous reviewer, whose comments greatly improved the clarity and focus of the paper. This work was partially financially supported by Russian Scientific Foundation (Grant RSF No. 14-27-00083).

Appendix A. Supplementary data

Supplementary data related to this article can be found at http://dx.doi.org/10.1016/j.gsf.2017.04.008.

References

Arzhannikov, S.G., Alekseev, S.V., Glyzin, A.V., Kulagina, N.V., Ignatova, N.V., Orlova, L.A., 2010. The Late Pleistocene–Holocene climate history in the western Todzha basin. Geology and Geophysics 51 (2), 206–221 (in Russian).

Binney, H., Edwards, M., Macias-Fauria, M., Lozhkin, A., Anderson, P., Kaplan, J.O., Andreev, A., Bezrukova, E., Blyakharchuk, T., Jankovska, V., Khazina, I., Krivonogov, S., Kremenetski, K., Nield, J., Novenko, E., Ryabogina, N., Solovieva, N., Willis, K., Zernitskaya, V., 2017. Vegetation of Eurasia from the last glacial maximum to present: key biogeographic patterns. Quaternary Science Reviews 157, 80–97.

Black, R.F., 1965. Ice wedge casts of Wisconsin. Wisconsin Academy of Science, Arts and Letters 54, 187–222.

Climatic data of the USSR, 1966. Buryatia and Chita Region, vol. 23(2). Gidrometeoizdat, Leningrad, 319 pp. (in Russian).

Feng, Z.-D., Ma, Y.Z., Zhang, H.C., Narantsetsega, T., Zhang, X.S., 2013. Holocene climate variations retrieved from Gun Nuur lake-sediment core in the northern Mongolian Plateau. The Holocene 23, 1721–1730.

French, H.M., Heginbottom, J.A. (Eds.), 1983. Guidebook to Permafrost and Related Features of the Northern Yukon Territory and Mackenzie Delta, Canada. University of Alaska, Alaska, 186 pp.

French, H., Shur, Y., 2010. The principles of cryostratigraphy. Earth-Science Reviews 101 (3–4), 190–206.

Fritz, M., Wolter, J., Rudaya, N., Palagushkina, O., Nazarova, L., Obu, J., Rethemeyer, J., Lantuit, H., Wetterich, S., 2016. Holocene ice-wedge polygon development in northern Yukon permafrost peatlands (Canada). Quaternary Science Reviews 147, 279–297.

Gavrilova, M.K., 1967. Microclimate and thermal regime of the surface and soils in the Chara Basin. In: Nekrasov, I.A. (Ed.), Geocryological Conditions of Transbaikalia and the Baikal Region. Nauka Publ. House, Moscow, pp. 148–161 (in Russian).

Jin, H.J., Chang, X.L., Luo, D.L., He, X.R., Lü, L.Z., Yang, Z.S., Guo, D.X., Chen, M.X., Harris, S., 2016. Evolution of permafrost in Northeast China since the Late Pleistocene. Sciences in Cold and Arid Regions 8 (4), 0269–0296. http://dx.doi.org/10.3724/SP.J.1226.2016.00269.

Johnsson, G., 1982. Localities visited on excursions during the Nordic Symposium on Frozen Ground Morphology. Geografisk Tidsskrift 82 (1), 99–103.

Klimovsky, I.V., Vasil'ieva, L.M., 1967. Palynological analysis of Quaternary sediments in Chara Basin containing soil and ice wedges. In: Nekrasov, I.A. (Ed.), Geocryological Conditions of Transbaikalia and the Baikal Region. Nauka Publ. House, Moscow, pp. 212–218 (in Russian).

Kolomyts, E.G., 1966. Geography features of snow in eastern Stanovoy highlands. In: Grave, N.A., Nekrasov, I.A. (Eds.), Geocryological Conditions of Transbaikalian North. Nauka Publ. House, Moscow, pp. 55–67 (in Russian).

Lopatin, D.V., 1967. On some peculiarities of the polygonal landforms development in the Chara Basin. In: Nekrasov, I.A. (Ed.), Geocryological Conditions of Transbaikalia and the Baikal Region. Nauka Publ. House, Moscow, pp. 205–212 (in Russian).

Meyer, H., Schönicke, L., Wand, U., Hubberten, H.-W., Friedrichsen, H., 2000. Isotope studies of hydrogen and oxygen in ground ice-experiences with the equilibration technique. Isotopes in Environmental and Health Studies 36, 133–149.

Murton, J.B., Kolstrup, E., 2003. Ice-wedge casts as indicators of paleotemperatures: precise proxy or wishful thinking. Progress in Physical Geography 27 (2), 155–170.

Nekrasov, I.A., Golovanova, G.V., 1966. Permafrost features near Upper Chara thermal spring. In: Grave, N.A., Nekrasov, I.A. (Eds.), Geocryological Conditions of Transbaikalian North. Nauka Publ. House, Moscow, pp. 172–180 (in Russian).

Nekrasov, I.A., Zabolotnik, S.I., 1967. Temperature regime and permafrost thickness of northern foothills in Udokan Ridge. In: Nekrasov, I.A. (Ed.), Geocryological Conditions of Transbaikalia and the Baikal Region. Nauka Publ. House, Moscow, pp. 124–135 (in Russian).

Opel, T., Dereviagin, A.Y., Meyer, H., Schirrmeister, L., Wetterich, S., 2011. Palaeoclimatic information from stable water isotopes of Holocene ice wedges on the Dmitrii Laptev Strait, northeast Siberia, Russia. Permafrost and Periglacial Processes 22 (1), 84–100.

Osadchy, S.S., 1982. Ice wedge in East Sayan and their stratigraphic significance. In: Late Pleistocene and Holocene in South of East Siberia. Nauka Publ. House, Novosibirsk, pp. 146–155.

Plyukhin, B.V., 1990. Udokan. Climatic Features and Atmosphere Protection. Nauka Publ. House, Novosibirsk, 109 pp. (in Russian).

Popp, S., Diekmann, B., Meyer, H., Siegert, C., Syromyatnikov, I., Hubberten, H.W., 2006. Palaeoclimate signals as inferred from stable-isotope composition of ground ice in Verkhoyansk foreland, Central Yakutia. Permafrost and Periglacial Processes 17, 119–132.

Reimer, P.J., Bard, E., Bayliss, A., Beck, J.W., Blackwell, P.G., Bronk Ramsey, C., Buck, C.E., Cheng, H., Edwards, R.L., Friedrich, M., Grootes, P.M., Guilderson, T.P., Haflidason, H., Hajdas, I., Hatté, C., Heaton, T.J., Hoffmann, D.L., Hughen, K.A., Kaiser, K.F., Kromer, B., Manning, S.W., Niu, M., Reimer, R.W., Richards, D.A., Scott, E.M., Southon, J.R., Staff, R.A., Turney, C.S.M., van der Plicht, J., Hogg, A., 2013. IntCal13 and Marine13 radiocarbon age calibration curves 0-50,000 years cal BP. Radiocarbon 55 (4), 1869–1887.

Romanovsky, N.N., Zaitsev, V.N., Volchenkov, S.Y., Volkova, V.E., Lisitsina, O.M., 1988. New data on permafrost of kodar-Chara-Udokan region. In: Senneset, K. (Ed.), Proceedings of the Fifth International Conference on Permafrost. Tapir Publishers, Trondheim. Norway, pp. 233–236.

Romanovsky, V.E., Drozdov, D.S., Oberman, N.G., Malkova, G.V., Kholodov, A.L., Marchenko, S.S., Moskalenko, N.G., Sergeev, D.O., Ukraintseva, N.G., Abramov, A.A., Gilichinsky, D.A., Vasiliev, A.A., 2010. Thermal state of permafrost in Russia. Permafrost and Periglacial Processes 21, 136–155. http://dx.doi.org/10.1002/ppp.683.

Sergeev, D.O., Stanilovskaya, J.V., Perlshtein, G.Z., Romanovsky, V.E., Bezdelova, A.P., Alexutina, D.M., Bolotyuk, M.M., Khimenkov, A.N., Kapralova, V.N., Motenko, R.G., Maleeva, A.N., 2016. Background geocryological monitoring in Northern Transbaikalia Region. Earth's Cryosphere 3 (XX), 23–31.

Sun, A., Feng, Z., 2013. Holocene climatic reconstructions from the fossil pollen record at Qigai Nuur in the southern Mongolian Plateau. The Holocene 23 (10), 1391–1402. http://dx.doi.org/10.1177/0959683613489581.

Tian, F., Cao, X., Dallmeyer, A., Zhao, Y., Nie, J., Herzschuh, U., 2017. Pollen-climate relationships in time (9 ka, 6 ka, 0 ka) and space (upland vs. lowland) in eastern continental Asia. Quaternary Science Reviews 156, 1–11.

Vaikmäe, R.A., Vasil'chuk, Y.K., 1991. Oxygen Isotope Analysis of Ground Ice on the North of Western Siberia, Yakutia and Chukotka. Estonia Institute of Geology publ., Tallinn, 70 pp. (in Russian).

Vasil'chuk, Y.K., 1992. Oxygen Isotope Composition of Ground Ice (Application to Paleogeocryological Reconstructions), vol. 1. Russian Academy of Sciences and Moscow University Publ, Moscow (420 pp.) and 2 (264 pp.) (in Russian).

Vasil'chuk, Y.K., 2006. Ice Wedge: Heterocyclity, Heterogeneity, Heterochroneity. Moscow University Press, Moscow, 404 pp. (in Russian).

Vasil'chuk, A.C., 2016. Pollen spectra of succession stages in arctic and subartic tundra. Arctic and Antarctic 1, 32–39. http://dx.doi.org/10.7256/2453-8922.2016.1.21367 (in Russian).

Vasil'chuk, Y.K., Kotlyakov, V.M., 2000. Principles of Isotope Geocryology and Glaciology. A Comprehensive Textbook. Moscow University Press, Moscow, 616 pp. (in Russian).

Vasil'chuk, Y.K., Vasil'chuk, A.C., 1995. Ice-wedge formation in Northern Asia during the Holocene. Permafrost and Periglacial Processes 6 (3), 273–279.

Vasil'chuk, Y.K., van der Plicht, J., Jungner, H., Vasil'chuk, A.C., 2000. AMS-dating of Late Pleistocene and Holocene syngenetic ice-wedges. Nuclear Instruments and Methods in Physics Research. Section B: Beam Interactions with Materials and Atoms 172, 637–641.

Vasil'chuk, Y.K., Zaitsev, V.N., Vasil'chuk, A.C., 2006. A ^{14}C-dating and oxygen-isotope diagram of a Holocene ice wedge on the Chara river (Transbaikal Region). Transactions (Doklady) of the Russian Academy of Sciences. Earth Science Section 407 (2), 265–270.

Vasil'chuk, A.C., 2007. Palynology and Chronology of Polygonal Ice Wedge Complexes in Russia Permafrost Area. Moscow University Press, Moscow, 488 pp. (in Russian).

Vasil'chuk, Y.K., 2013. Syngenetic ice wedges: cyclical formation, radiocarbon age and stable-isotope records. Permafrost and Periglacial Processes 24 (1), 82–93.

Vasil'chuk, Y.K., Alexeev, S.V., Arzhannikov, S.G., Papesch, W., Rank, D., Vasil'chuk, A.C., 2002. First data on isotopic dating of Holocene syngenetic ice wedges from the Myorzlyi Yar area, Upper reaches of Yenisei River. Doklady Earth Sciences 383 (2), 225–229.

Weather in Russia. http://meteo.infospace.ru (in Russian).

Yang, S., Jin, H., 2011. $\delta^{18}O$ and δD records of inactive ice wedge in Yitulihe, Northeastern China and their paleoclimatic implications. Science China Earth Sciences 54, 119–126. http://dx.doi.org/10.1007/s11430-010-4029-5.

Yang, Y.Z., Wu, Q.B., Yun, H.B., 2013. Stable isotope variations in the ground ice of Beiluhe Basin on the Qinghai-Tibet Plateau. Quaternary International 313–314, 85–91. http://dx.doi.org/10.1016/j.quaint.2013.07.037.

Yang, S., Cao, X., Jin, H., 2015. Validation of ice-wedge isotopes at Yitulihe, northeastern China as climate proxy. Boreas 44 (3), 502–510. http://dx.doi.org/10.1111/bor.12121.

Yang, Y., Wu, Q., Jiang, G., Zhang, P., 2016. Stable isotopic stratification and growth patterns of ground ice in permafrost on the Qinghai-Tibet Plateau, China. Permafrost and Periglacial Processes. http://dx.doi.org/10.1002/ppp.1892 (in press).

Zabolotnik, S.I., Klimovsky, I.V., 1966. Seasonal soil freezing and thawing in the Chara Basin. In: Nekrasov, I.A. (Ed.), Geocryological Conditions of Transbaikalia and the Baikal Region. Nauka Publ. House, Moscow, pp. 162–171 (in Russian).

Zhao, C., Li, X., Zhou, X., Zhao, K., Yang, Q., 2016. Holocene vegetation succession and responses to climate change in the northern sector of Northeast China. Science China Earth Sciences 59, 1390–1400. http://dx.doi.org/10.1007/s11430-015-5239-7.